# Motion Predicts Clinical Callus Formation

## Construct-Specific Finite Element Analysis of Supracondylar Femoral Fractures

Jacob Elkins, MD, PhD, J. Lawrence Marsh, MD, Trevor Lujan, PhD, Richard Peindl, PhD, James Kellam, MD, Donald D. Anderson, PhD, and William Lack, MD

*Investigation performed at the Department of Orthopaedics and Rehabilitation, University of Iowa Hospitals and Clinics, Iowa City, Iowa, and the Department of Orthopaedic Surgery, Carolinas Medical Center, Charlotte, North Carolina*

**Background:** Mechanotransduction is theorized to influence fracture-healing, but optimal fracture-site motion is poorly defined. We hypothesized that three-dimensional (3-D) fracture-site motion as estimated by finite element (FE) analysis would influence callus formation for a clinical series of supracondylar femoral fractures treated with locking-plate fixation.

**Methods:** Construct-specific FE modeling simulated 3-D fracture-site motion for sixty-six supracondylar femoral fractures (OTA/AO classification of 33A or 33C) treated at a single institution. Construct stiffness and directional motion through the fracture were investigated to assess the validity of construct stiffness as a surrogate measure of 3-D motion at the fracture site. Callus formation was assessed radiographically for all patients at six, twelve, and twenty-four weeks postoperatively. Univariate and multivariate linear regression analyses examined the effects of longitudinal motion, shear (transverse motion), open fracture, smoking, and diabetes on callus formation. Construct types were compared to determine whether their 3-D motion profile was associated with callus formation.

**Results:** Shear disproportionately increased relative to longitudinal motion with increasing bridge span, which was not predicted by our assessment of construct stiffness alone. Callus formation was not associated with open fracture, smoking, or diabetes at six, twelve, or twenty-four weeks. However, callus formation was associated with 3-D fracture-site motion at twelve and twenty-four weeks. Longitudinal motion promoted callus formation at twelve and twenty-four weeks ($p = 0.017$ for both). Shear inhibited callus formation at twelve and twenty-four weeks ($p = 0.017$ and $p = 0.022$, respectively). Titanium constructs with a short bridge span demonstrated greater longitudinal motion with less shear than did the other constructs, and this was associated with greater callus formation ($p < 0.001$).

**Conclusions:** In this study of supracondylar femoral fractures treated with locking-plate fixation, longitudinal motion promoted callus formation, while shear inhibited callus formation. Construct stiffness was found to be a poor surrogate of fracture-site motion. Future implant design and operative fixation strategies should seek to optimize 3-D fracture-site motion rather than rely on surrogate measures such as axial stiffness.

**Peer Review:** This article was reviewed by the Editor-in-Chief and one Deputy Editor, and it underwent blinded review by two or more outside experts. The Deputy Editor reviewed each revision of the article, and it underwent a final review by the Editor-in-Chief prior to publication. Final corrections and clarifications occurred during one or more exchanges between the author(s) and copyeditors.

Locking plates are frequently used in bridge-plate fixation of comminuted and osteoporotic supracondylar femoral fractures, emphasizing the preservation of blood supply over anatomic reduction[1,2]. Bridge plating requires secondary fracture-healing (callus formation), and there is concern that locked constructs may be too rigid, with many reports of deficient callus formation, delayed union, late implant failure, and nonunion involving locked plating of supracondylar femoral fractures[1,3-18]. The mechanical environment influences fracture-healing, and construct properties have been shown to affect both construct stiffness and callus formation[4-7,18-24]. These findings are influencing clinical practice, as screw technology has been developed

**Disclosure:** One or more of the authors received payments or services, either directly or indirectly (i.e., via his or her institution), from a third party in support of an aspect of this work. In addition, one or more of the authors, or his or her institution, has had a financial relationship, in the thirty-six months prior to submission of this work, with an entity in the biomedical arena that could be perceived to influence or have the potential to influence what is written in this work. Also, one or more of the authors has a patent or patents, planned, pending, or issued, that is broadly relevant to the work. No author has had any other relationships, or has engaged in any other activities, that could be perceived to influence or have the potential to influence what is written in this work. The complete **Disclosures of Potential Conflicts of Interest** submitted by authors are always provided with the online version of the article.

**TABLE I Clinical Characteristics of the Patient Cohort***

| | |
|---|---|
| Age† *(yr)* | 63 (49 to 66) |
| Female‡ | 48 (72.7%) |
| Open fracture‡ | 15 (22.7%) |
| Smoking‡ | 18 (27.3%) |
| Diabetes‡ | 16 (24.2%) |

*N = 66 supracondylar femoral fractures. †The values are given as the median with the interquartile range in parentheses. ‡The values are given as the number, with the percentage in parentheses.

to increase interfragmentary motion and has been found to increase callus formation in an animal model[22,24].

The amount of interfragmentary motion optimal for secondary fracture-healing is poorly defined. Three-dimensional (3-D) fracture-site motion includes longitudinal and transverse (shear) components, but quantifying 3-D fracture-site motion clinically remains impractical. Historically, ex vivo estimates of axial stiffness have been used as surrogate measures of fracture-site motion. However, studies conflict regarding the relationship of callus formation, construct parameters, axial stiffness, and fracture-site motion, suggesting that the relationship between axial stiffness and 3-D fracture-site motion is complex[18,19,23,24]. Therefore, determining the optimal mechanical environment for secondary fracture-healing is largely limited by an inability to measure or predict fracture-site motion.

Motion may be estimated through sophisticated ex vivo testing of fixation constructs. However, given the complexities of such investigations, as well as the desire for parametric testing of surgeon-controlled construct variables, experimental testing is logistically prohibitive. Furthermore, laboratory testing is limited to existing implants. Conversely, computational modeling, specifically finite element (FE) analysis, permits parametric investigation at a fraction of the economic cost. Such computational analysis has been proposed as a tool by which fracture-healing may be studied in the setting of various orthopaedic treatments and allows pre-production analysis of implant design[25,26].

In summary, the biomechanical environment is theorized to influence fracture-healing, but optimal fracture-site motion is poorly defined. Axial stiffness has been used as a surrogate measure of fracture-site motion, but its relationship to directional fracture-site motion and its effect on clinical healing are unclear. Combining a technique of radiographic callus assessment with clinical construct-specific computational modeling would allow the study of mechanotransduction in clinical fracture-healing[25-27].

The objective of our study was to assess whether 3-D fracture-site motion, as predicted by construct-specific FE analysis, would influence callus formation in a clinical series of supracondylar femoral fractures. We hypothesized that longitudinal fracture-site motion would promote callus formation, while transverse motion (shear) would be inhibitory. We further studied whether construct stiffness was a suitable surrogate measure of 3-D fracture-site motion. We sought to identify the construct parameters most influential in secondary fracture-healing by examining the relationship of construct parameters to fracture-site motion and clinical callus formation.

## Materials and Methods

### *FE Analysis*

We developed a 3-D FE model of a comminuted supracondylar femoral fracture that could be varied to allow construct-specific modeling of clinical cases treated at a single institution (Fig. 1). The model consisted of two components: osseous anatomy and fixation hardware. Osseous anatomy was obtained from manual segmentation of the National Library of Medicine (NLM) Visible Human Male data set. The Visible Human Project is an extension of the NLM's 1986 Long-Range Plan, providing detailed 3-D representations of normal male and female anatomy[28]. A virtual supracondylar femoral fracture was simulated using Geomagic software (Geomagic). The geometry for a thirteen-hole fixation plate was obtained by manually digitizing and averaging measurements from four thirteen-hole distal femoral locking-plate implants (Synthes, Smith & Nephew, Zimmer, and DePuy) to create a generic plate. The osseous anatomy was meshed with standard hexahedral elements using TrueGrid meshing software (XYZ Scientific Applications). The plate was meshed with hexahedral elements within Abaqus/CAE (Complete Abaqus Environment) software (Dassault Systèmes) and registered with the osseous anatomy.

Screws coincident with screw-holes in the plate were generated in TrueGrid using hexahedral elements. Screw fixation was simulated by specifying contact constraints between the surface of the screws and the surface of the bone and plates, with a friction coefficient of 0.5. The plate was simulated as linear elastic stainless steel (Young modulus, E = 210 GPa; Poisson ratio, $\nu$ = 0.3) or titanium (E = 110 GPa; $\nu$ = 0.3). Cortical bone was modeled as linear elastic (E = 17 GPa; $\nu$ = 0.3). For all simulations, the distal articular surface was rigidly fixed, and an axial load of 1200 N was applied over 0.1 second to the center of the femoral head to simulate single-limb stance. This resulted in displacement of the proximal part of the femur and a narrowing of the fracture gap. All FE simulations were performed as quasistatic using Abaqus/Explicit 6.10.

### *Modeling the Clinical Case Series*

We used a model that simulated construct-specific mechanical loading of sixty-six supracondylar femoral fractures treated at a single institution. Plate material was varied to simulate the construct for each clinical case (thirty-three stainless steel and thirty-three titanium constructs). Proximal fixation was varied to study the entire range of bridge spans from the case series (20 to 180 mm). The bridge span was determined as the Euclidean distance between the two nearest screws proximal and distal to the fracture site. We ran simulations that included material properties for both stainless steel and titanium constructs.

### *Validation of FE-Predicted Axial Stiffness and Fracture-Site Motion*

The results of our FE analysis were validated using fourth-generation Sawbones femoral specimens (Pacific Research Laboratories). Distal femoral locking

**TABLE II Univariate Linear Regression Analysis of Callus Formation**

| | P Value | | |
|---|---|---|---|
| | 6 Wk | 12 Wk | 24 Wk |
| Open fracture | 0.344 | 0.158 | 0.532 |
| Smoking | 0.398 | 0.119 | 0.229 |
| Diabetes | 0.679 | 0.921 | 0.850 |
| Longitudinal motion | 0.271 | 0.455 | 0.403 |
| Shear | 0.295 | 0.761 | 0.889 |

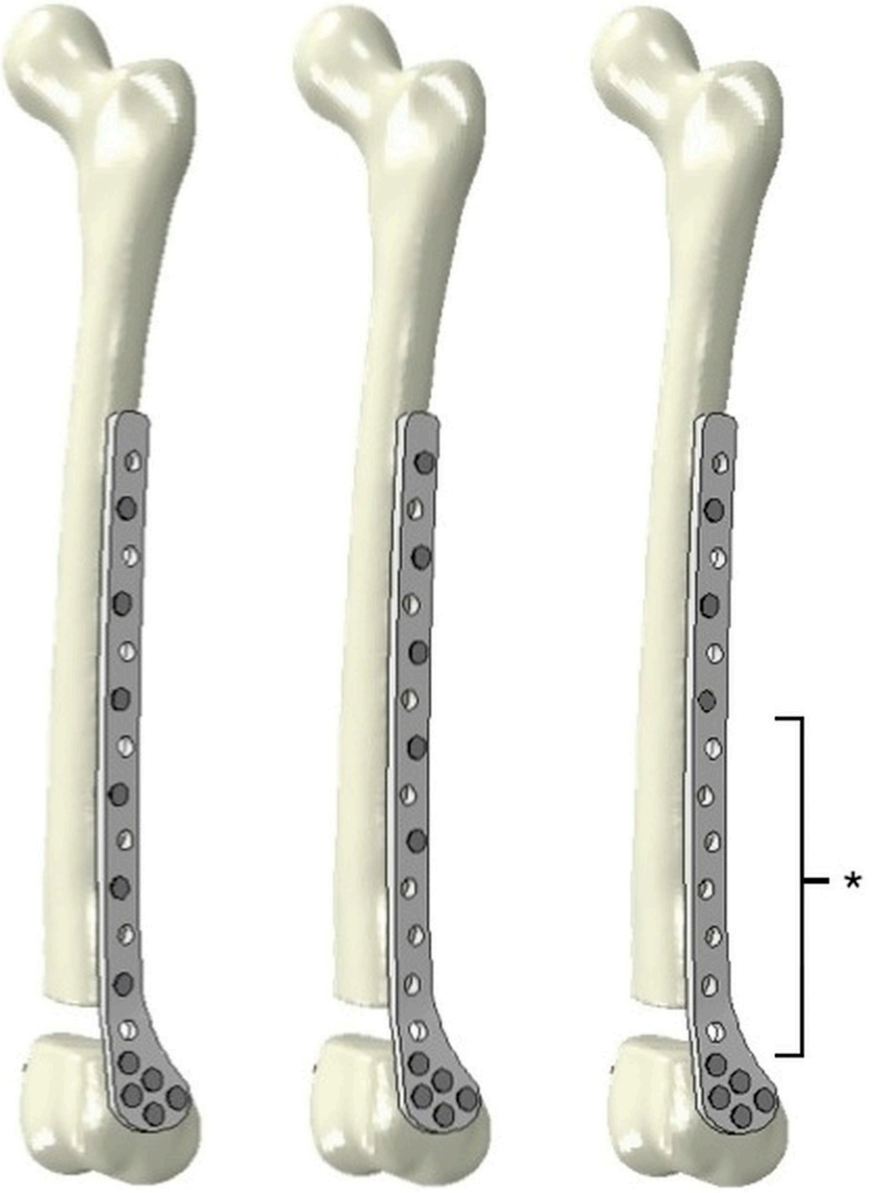


Fig. 1

The FE model consisted of osseous anatomy and a thirteen-hole distal femoral locking plate. Three examples of varied bridge span are shown, where the bridge span (*) was determined as the Euclidean distance between the two nearest screws proximal and distal to the fracture site.

plates were secured to the lateral surface of the femoral specimens by an orthopaedic trauma surgeon. Following the application of each construct, a 15-mm section of the supracondylar region of the distal femoral specimens was resected to simulate a comminuted fracture. Three distal femoral fracture implant systems were tested, with separate Sawbones specimens used for each implant system: (1) the titanium alloy Non-Contact Bridging (Ti NCB) Polyaxial Locking Plate System (Zimmer), (2) the titanium alloy Less Invasive Stabilization System (Ti LISS) Plate (Synthes), and (3) the stainless steel alloy LISS (SSt LISS) Plate (Synthes).

Axial loading (0 to 1200 N) was applied such that the force vector went through the center of the femoral head and was directed toward the intercondylar notch (simulating single-limb stance). A custom load frame consisting entirely of nonmagnetic material components was constructed to permit use of a trakSTAR 3-D tracking system (Ascension Technology) to monitor the position of the proximal and distal osteotomy surfaces under loaded and unloaded conditions. Axial stiffness and fracture-site motion were recorded for varying bridge spans for each implant system.

### *Callus Assessment in the Clinical Series*

A power analysis using a two-sample Student t test estimated that a sample size of fifty would be needed to achieve 85% power in detecting a 50% difference in callus formation at twelve weeks. Sixty-six supracondylar femoral fractures (OTA/AO classification, 33A or 33C)[29] treated with locking-plate fixation at a single institution were assessed for periosteal callus formation at six, twelve, and twenty-four weeks. This case series[18] and the technique of radiographic callus assessment[27] were previously described. However, the analysis of fracture-site motion, which was the goal of the present study, had not been previously conducted. Custom software was used to objectively measure callus area ($mm^2$) from the medial,

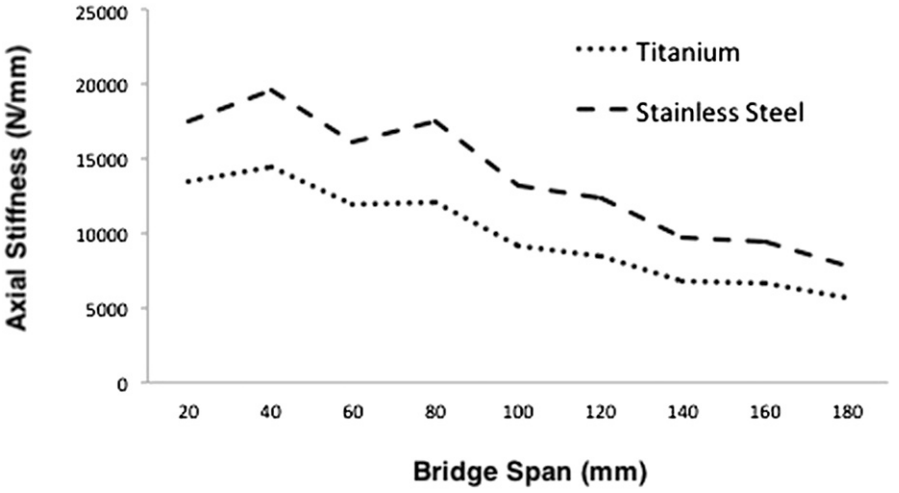


Fig. 2

Axial stiffness as predicted by FE analysis. Axial stiffness decreased with increasing bridge span and when changing the model from a stainless steel to a titanium construct material.

anterior, and posterior cortices on digital radiographs, without requiring manual tracing of the callus boundaries. This software measured callus in surrogate models with an error rate of <5%, and these measurements of clinical callus formation correlated extremely well with an independent analysis by orthopaedic surgeons ($r^2 = 0.94$; $p < 0.001$)[27]. Finally, three orthopaedic clinicians (two orthopaedic trauma surgeons and one resident) independently verified the callus boundaries assigned by the software for all sixty-six cases analyzed in this study.

### *Statistical Analysis*

Univariate and multivariate linear regression analyses were performed to analyze the associations of longitudinal motion, transverse motion, patient factors (smoking and diabetes), and injury (open versus closed fracture) with callus formation. The findings of the multivariate linear regression analysis were used to select the construct from the clinical case series that best exhibited a 3-D motion profile that would promote callus. A t test was performed for statistical comparison of callus formation at six, twelve, and twenty-four weeks between this best construct and the other constructs in the clinical series. Significance required a p value of ≤0.05.

### *Source of Funding*

Materials necessary for validation of the FE model were obtained through a Zimmer in-kind material grant and a Synthes research grant.

## Results

### *Construct Stiffness Fails to Predict 3-D Motion Through the Fracture*

Decreasing axial stiffness as predicted by FE analysis was associated with increasing total motion through the fracture site (Figs. 2 and 3). However, the direction of motion was highly dependent on bridge span and could not be predicted from axial stiffness alone. Although varying the construct material in the model altered the axial stiffness and affected longitudinal and transverse motion similarly, increasing bridge span by placing the proximal screws farther from the fracture disproportionately increased transverse motion (shear) at the fracture

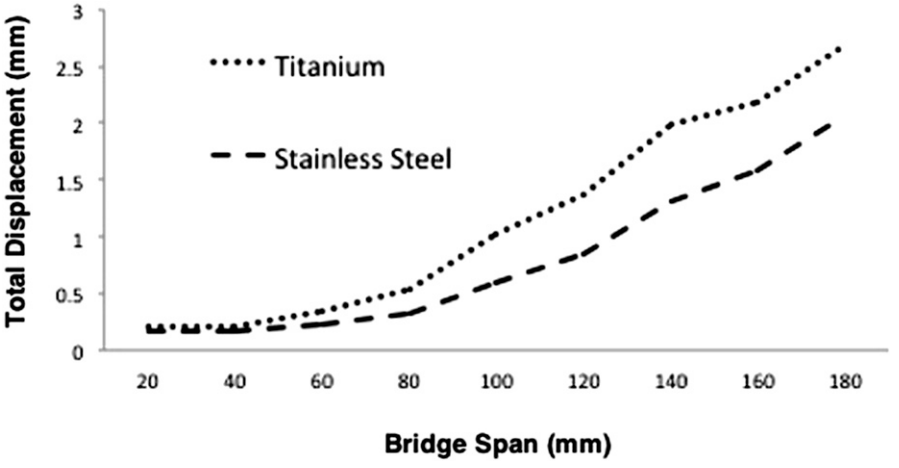


Fig. 3

Total displacement as predicted by FE analysis. Total motion at the fracture site increased with increasing bridge span and when changing the model from a stainless steel to a titanium construct material (inverse relationship to axial stiffness).

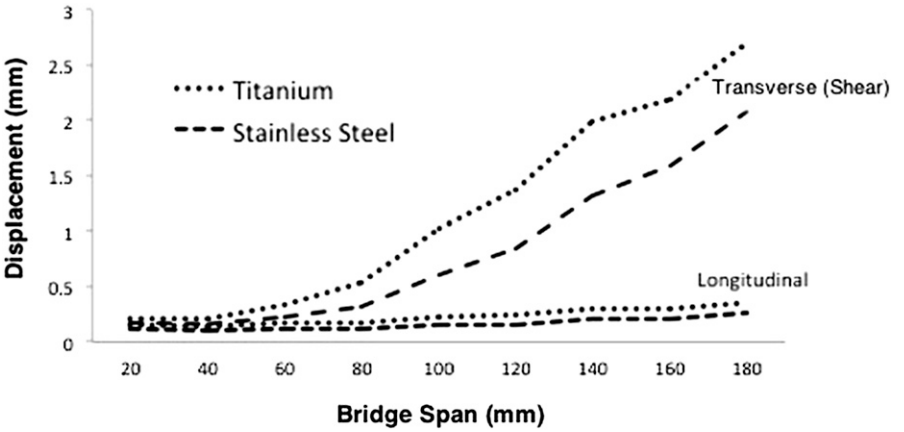


Fig. 4

Three-dimensional motion as predicted by FE analysis. An analysis of 3-D motion demonstrated that increasing bridge span caused increased total motion at the fracture site, primarily through a dramatic increase in shear relative to longitudinal motion. Varying the model by construct material, however, had a more balanced effect on both longitudinal motion and shear.

site (Fig. 4). Constructs with a bridge span of >80 mm were increasingly dominated by shear, regardless of construct material.

### *Validation of FE Analysis*

The FE-predicted relationship of construct material and bridge span to 3-D fracture-site motion was confirmed with the Sawbones testing (Fig. 5). Specifically, as bridge span increased for both titanium and stainless steel constructs, fracture-site motion was dominated by shear with very little effect on longitudinal motion. Shear became dominant for bridge spans of >80 mm, similar to the prediction of the FE analysis.

### *Characteristics of the Clinical Cohort*

The cohort consisted of sixty-four adult patients with a total of sixty-six supracondylar femoral fractures treated with locking-plate fixation. The cases studied in this clinical series were treated with bridge-plate fixation. The median age was sixty-three years. There were forty-eight females (72.7% of the fractures), eighteen smokers (27.3%), and sixteen patients with diabetes (24.2%). There were fifteen open fractures (22.7%). The clinical characteristics of the cohort are presented in Table I.

### *Univariate and Multivariate Analyses of Callus Formation*

The results of the univariate analysis are presented in Table II. There was no association between callus formation and open fracture, smoking, diabetes, longitudinal motion, or shear at six, twelve, or twenty-four weeks. However, on multivariate analysis (Table III), we found a significant association between callus formation and longitudinal motion and shear at twelve and twenty-four weeks. Longitudinal motion promoted callus formation (a positive standardized regression coefficient) at twelve and twenty-four weeks ($p = 0.017$ for both). Shear demonstrated an inhibitory effect (a negative standardized regression coefficient) at twelve and twenty-four weeks ($p = 0.017$ and $p = 0.022$, respectively).

### *Constructs Favoring Callus Formation*

Titanium constructs with a short bridge span (≤80 mm) were used for twenty-two of the sixty-six fractures, and they demonstrated

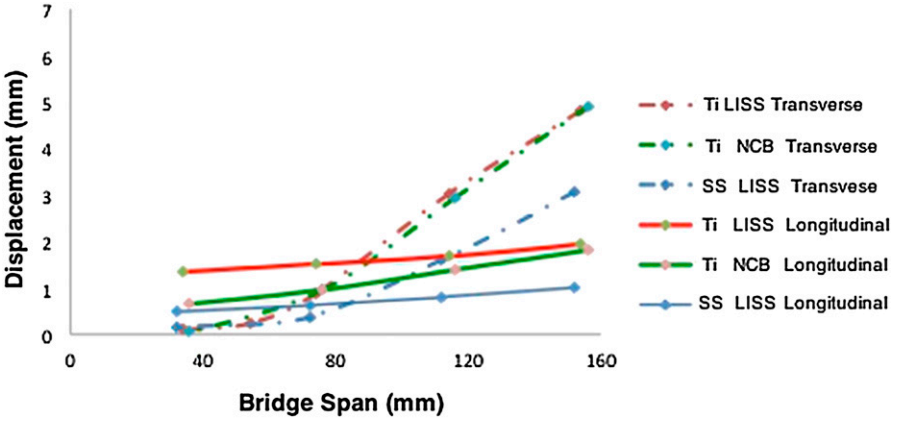


Fig. 5

Sawbones testing confirmed the predictions of FE analysis. Increasing bridge span led to an unbalanced increase in shear (transverse motion) relative to longitudinal motion through the fracture site, while varying the model by construct material more equally affected shear and longitudinal motion.

**TABLE III Multivariate Linear Regression Analysis of Callus Formation**

| | 6 Wk | | 12 Wk | | 24 Wk | |
|---|---|---|---|---|---|---|
| | Coefficient (95% CI)* | P Value | Coefficient (95% CI)* | P Value | Coefficient (95% CI)* | P Value |
| Open fracture | 0.178 (−0.112 to 0.468) | 0.224 | 0.154 (−0.113 to 0.422) | 0.251 | 0.045 (−0.234 to 0.324) | 0.747 |
| Smoking | −0.131 (−0.402 to 0.140) | 0.336 | −0.190 (−0.446 to 0.067) | 0.144 | −0.145 (−0.416 to 0.126) | 0.287 |
| Diabetes | −0.148 (−0.440 to 0.144) | 0.314 | −0.090 (−0.356 to 0.176) | 0.5 | −0.030 (−0.311 to 0.251) | 0.831 |
| Longitudinal motion | 0.080 (−0.504 to 0.665) | 0.784 | 0.814 (0.149 to 1.479) | 0.017† | 0.813 (0.149 to 1.478) | 0.017† |
| Shear | 0.078 (−0.508 to 0.663) | 0.792 | −0.811 (−1.474 to −0.148) | 0.017† | −0.784 (−1.449 to −0.118) | 0.022† |

*The values are presented as the standardized regression coefficient. A positive value indicates that callus area increased with the presence or magnitude of the parameter, and a negative value indicates that the callus area decreased. The absolute magnitude of the coefficient reflected the magnitude of the effect. CI = confidence interval. †A significant association with callus formation.

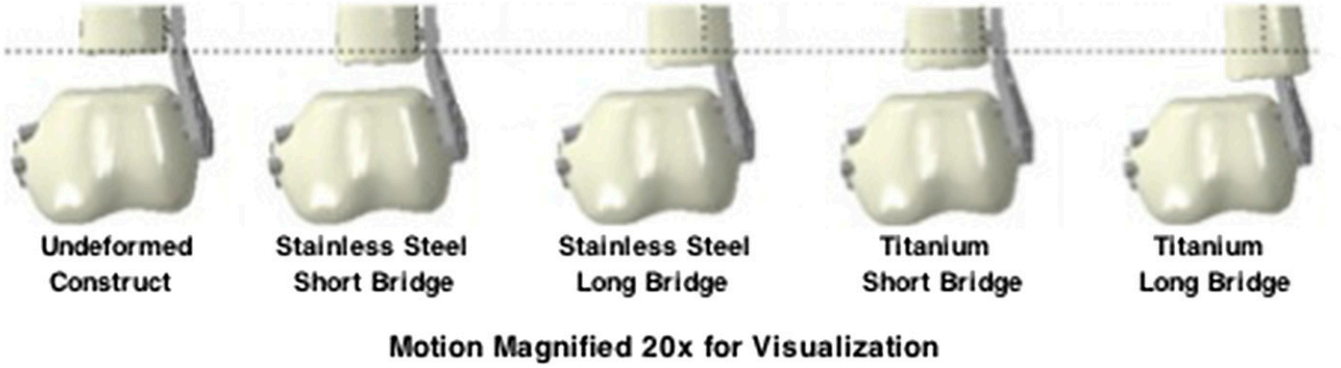


Fig. 6

The effect of construct properties on fracture-site motion is demonstrated visually. Longer bridge spans were associated with notably more transverse motion (shear) through the fracture. Titanium constructs with short bridge spans demonstrated greater longitudinal motion than stainless steel constructs and less transverse motion than constructs with long bridge spans.

greater longitudinal motion relative to transverse fracture-site motion when compared with the other constructs in the clinical case series, according to both FE analysis and Sawbones testing (Fig. 6, with ×20 magnification of motion for the purpose of visualization). For bridge spans of >80 mm, shear was increasingly dominant over longitudinal motion (Fig. 4). Given this predicted motion profile, multivariate regression analysis predicted that these constructs (favoring longitudinal motion over transverse motion) would therefore be associated with greater callus formation. This was found to be true, as the titanium constructs with a short bridge span (≤80 mm) demonstrated greater callus formation at six, twelve, and twenty-four weeks ($p < 0.05$) when compared with all other constructs (Fig. 7).

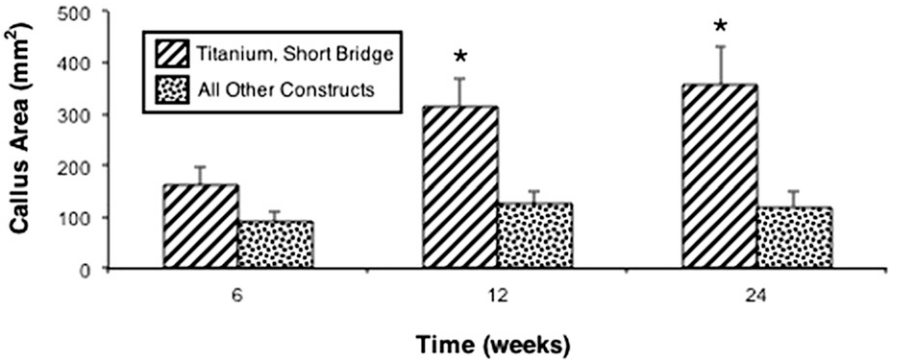


Fig. 7

Callus formation by construct over time. Titanium constructs with short bridge spans resulted in significantly greater callus area at twelve weeks (*$p < 0.001$) and twenty-four weeks (*$p < 0.001$). The error bars represent the standard error of the mean.

## Discussion

Computationally predicted overall fracture-site motion generally increased with decreasing axial stiffness. However, varying bridge span had a dramatically disparate effect on transverse (shear) versus longitudinal motion. This demonstrates that axial stiffness is a poor surrogate for the individual components of 3-D motion at the fracture site (longitudinal motion and shear). Furthermore, the components of 3-D fracture-site motion were each independently associated with clinical callus formation in this clinical case series of supracondylar femoral fractures treated with locking-plate fixation. This was observed on multivariate analysis, but not on univariate analysis. The lack of significance on univariate analysis appears to be due to the competing associations demonstrated between these factors and callus formation. Longitudinal motion was associated with greater callus formation, and shear, with lesser callus formation. Both forms of motion increased with decreasing construct stiffness, but to differing degrees, depending on the construct parameter that was being varied (i.e., material or screw position). These competing effects confounded each other on univariate analysis, and it was only with multivariate analysis that the two components of 3-D motion could be assessed for their independent effect.

Given that longitudinal motion and shear had competing effects on callus formation, we assessed the relationship between callus formation and the 3-D motion profile of a construct. Callus formation for constructs that maximized longitudinal motion relative to transverse motion on FE analysis (titanium constructs with a bridge span of ≤80 mm, Fig. 6) was compared with callus formation for all other cases in the series. Titanium constructs with a short bridge span (≤80 mm) demonstrated significantly greater callus at twelve and twenty-four weeks, and this disparity increased over time as healing progressed (Fig. 7). These results explain previous findings that demonstrated that plate material was significantly associated with callus formation, while increasing bridge span was not[18]. Increasing bridge span preferentially increased shear at the fracture, which we found to be inversely associated with callus formation.

This study is, to our knowledge, the first to demonstrate that construct-specific 3-D fracture-site motion, predicted computationally and validated experimentally, is predictive of callus formation in a clinical case series. The concept that 3-D motion is important to tissue differentiation and bone-healing has long been appreciated. Longitudinal interfragmentary strain was shown to increase the rate of bone-healing in a review of previous studies[30]. Transverse motion was suggested to negatively affect fracture-healing more than fifty years ago, and an inhibitory effect of shear and bending moments on healing has been demonstrated using in vivo animal models and in multiple computational investigations[31-36]. Interestingly, one of these computational investigations noted that loading associated with a bending moment predicted deficient and asymmetric callus due to asymmetric motion at the fracture site[36]. Analogous clinical results have also been reported for a clinical case series of distal femoral fractures treated with locked plating (an environment that includes a notable bending moment)[18]. Although many questions remain regarding the biologic mechanisms behind these findings, recent animal research has demonstrated that fracture fixation stability dictates the differentiation pathway of periosteal progenitor cells[37].

Three decades ago, transverse motion predicted by FE analysis suggested that longitudinal strain alone is inadequate for studying the mechanoregulation of fracture-healing[38]. Recent research has further questioned the use of uniaxial load-displacement relationships for the assessment of distal femoral constructs[39]. The present study demonstrated a positive association of longitudinal motion, and a negative association of transverse motion, with callus formation. The ability to predict callus formation is lost when ignoring the directionality of motion through the fracture. These findings agree with those of a previous study involving a sheep model of osteotomy, which found that bone-healing (as measured by callus formation and mechanical stability) was significantly reduced in the setting of shear[40].

This study had several limitations that must be recognized. The FE model examined single-limb stance, but future iterations might include a variety of loading conditions simulating additional clinical conditions. The simulations of clinical cases in this study varied bridge span and plate material only. In future iterations, the model could be adapted to include additional construct features, including variations in plate design. We limited our analysis of 3-D fracture-site motion to longitudinal and transverse motion; however, 3-D motion is defined by translation and rotation in three planes; a more robust analysis of 3-D motion could be accomplished in future studies. Assessment of fracture-site strain and potential contact interactions between fragments was limited in the current model by generic fracture geometry. It would be possible to customize the FE model with individual fracture geometry on the basis of clinical imaging, permitting analysis of the relationship between 3-D fracture-site strain and clinical callus formation. Furthermore, future studies would benefit from assessing the quality or density of the callus formed.

This study combined clinical data with construct-specific FE modeling to evaluate mechanotransduction theory. Technology has been developed to decrease construct stiffness and increase interfragmentary motion[22,24]. However, optimal interfragmentary strain is poorly defined, and the relative importance of fracture-site motion in achieving union remains unclear. Axial stiffness is commonly employed as a surrogate measure of fracture-site motion, and recommendations have been made for "biologic fixation" by controlling construct stiffness[19,20]. Our findings in the present study question the previously described technique of increasing bridge span to decrease construct stiffness[19]. This may unintentionally increase shear, thereby inhibiting callus formation. Although construct stiffness is associated with the magnitude of motion at the fracture, it is a poor surrogate for directionality of motion. Our clinical data demonstrated a significant relationship between 3-D fracture-site motion and callus formation, while no such relationship was found between axial stiffness and callus formation.

Although titanium constructs with a short bridge span were associated with greater callus formation, shorter bridge spans have also been associated with increased von Mises stress within such implants[41]. Therefore, these results do not support a specific fixation

strategy, but rather, add to our understanding of the relationship between fracture-site motion and callus formation. Future implant design and operative fixation strategies aimed toward maximizing secondary fracture-healing should seek to optimize 3-D fracture-site motion rather than rely on surrogate measures such as axial stiffness. ■

Jacob Elkins, MD, PhD[1]
J. Lawrence Marsh, MD[1]
Trevor Lujan, PhD[2]
Richard Peindl, PhD[3]
James Kellam, MD[4]
Donald D. Anderson, PhD[1]
William Lack, MD[5]

[1]Department of Orthopaedics and Rehabilitation, University of Iowa Hospitals and Clinics, Iowa City, Iowa

[2]Department of Mechanical and Biomedical Engineering, Boise State University, Boise, Idaho

[3]Department of Orthopaedic Surgery, Carolinas Medical Center, Charlotte, North Carolina

[4]Department of Orthopaedic Surgery, University of Texas Health Science Center, Houston, Texas

[5]Department of Orthopaedic Surgery and Rehabilitation, Loyola University Medical Center, Maywood, Illinois

## References

**1.** Kubiak EN, Fulkerson E, Strauss E, Egol KA. The evolution of locked plates. J Bone Joint Surg Am. 2006 Dec;88(Suppl 4):189-200.
**2.** Perren SM. Evolution of the internal fixation of long bone fractures. The scientific basis of biological internal fixation: choosing a new balance between stability and biology. J Bone Joint Surg Br. 2002 Nov;84(8):1093-110.
**3.** Egol KA, Kubiak EN, Fulkerson E, Kummer FJ, Koval KJ. Biomechanics of locked plates and screws. J Orthop Trauma. 2004 Sep;18(8):488-93.
**4.** Claes LE, Heigele CA, Neidlinger-Wilke C, Kaspar D, Seidl W, Margevicius KJ, Augat P. Effects of mechanical factors on the fracture healing process. Clin Orthop Relat Res. 1998 Oct;(355)(Suppl):S132-47.
**5.** Duda GN, Sollmann M, Sporrer S, Hoffmann JE, Kassi JP, Khodadadyan C, Raschke M. Interfragmentary motion in tibial osteotomies stabilized with ring fixators. Clin Orthop Relat Res. 2002 Mar;396:163-72.
**6.** Goodship AE, Kenwright J. The influence of induced micromovement upon the healing of experimental tibial fractures. J Bone Joint Surg Br. 1985 Aug;67 (4):650-5.
**7.** Augat P, Penzkofer R, Nolte A, Maier M, Panzer S, v Oldenburg G, Pueschl K, Simon U, Bühren V. Interfragmentary movement in diaphyseal tibia fractures fixed with locked intramedullary nails. J Orthop Trauma. 2008 Jan;22(1):30-6.
**8.** Uhthoff HK, Poitras P, Backman DS. Internal plate fixation of fractures: short history and recent developments. J Orthop Sci. 2006 Mar;11(2):118-26.
**9.** Henderson CE, Bottlang M, Marsh JL, Fitzpatrick DC, Madey SM. Does locked plating of periprosthetic supracondylar femur fractures promote bone healing by callus formation? Two cases with opposite outcomes. Iowa Orthop J. 2008;28: 73-6.
**10.** Ring D, Kloen P, Kadzielski J, Helfet D, Jupiter JB. Locking compression plates for osteoporotic nonunions of the diaphyseal humerus. Clin Orthop Relat Res. 2004 Aug;425:50-4.
**11.** Button G, Wolinsky P, Hak D. Failure of less invasive stabilization system plates in the distal femur: a report of four cases. J Orthop Trauma. 2004 Sep;18 (8):565-70.
**12.** Sommer C, Gautier E, Müller M, Helfet DL, Wagner M. First clinical results of the Locking Compression Plate (LCP). Injury. 2003 Nov;34(Suppl 2):B43-54.
**13.** Fankhauser F, Gruber G, Schippinger G, Boldin C, Hofer HP, Grechenig W, Szyszkowitz R. Minimal-invasive treatment of distal femoral fractures with the LISS (Less Invasive Stabilization System): a prospective study of 30 fractures with a follow up of 20 months. Acta Orthop Scand. 2004 Feb;75(1):56-60.
**14.** Ricci WM, Loftus T, Cox C, Borrelli J. Locked plates combined with minimally invasive insertion technique for the treatment of periprosthetic supracondylar femur fractures above a total knee arthroplasty. J Orthop Trauma. 2006 Mar;20 (3):190-6.
**15.** Herrera DA, Kregor PJ, Cole PA, Levy BA, Jönsson A, Zlowodzki M. Treatment of acute distal femur fractures above a total knee arthroplasty: systematic review of 415 cases (1981-2006). Acta Orthop. 2008 Feb;79(1):22-7.
**16.** Schütz M, Müller M, Regazzoni P, Höntzsch D, Krettek C, Van der Werken C, Haas N. Use of the less invasive stabilization system (LISS) in patients with distal femoral (A033) fractures: a prospective multicenter study. Arch Orthop Trauma Surg. 2005 Mar;125(2):102-8. Epub 2005 Feb 2.
**17.** Henderson CE, Kuhl LL, Fitzpatrick DC, Marsh JL. Locking plates for distal femur fractures: is there a problem with fracture healing? J Orthop Trauma. 2011 Feb;25 (Suppl 1):S8-14.
**18.** Lujan TJ, Henderson CE, Madey SM, Fitzpatrick DC, Marsh JL, Bottlang M. Locked plating of distal femur fractures leads to inconsistent and asymmetric callus formation. J Orthop Trauma. 2010 Mar;24(3):156-62.
**19.** Stoffel K, Dieter U, Stachowiak G, Gächter A, Kuster MS. Biomechanical testing of the LCP—how can stability in locked internal fixators be controlled? Injury. 2003 Nov;34(Suppl 2):B11-9.
**20.** Field JR, Törnkvist H, Hearn TC, Sumner-Smith G, Woodside TD. The influence of screw omission on construction stiffness and bone surface strain in the application of bone plates to cadaveric bone. Injury. 1999 Nov;30(9):591-8.
**21.** Stoffel K, Lorenz KU, Kuster MS. Biomechanical considerations in plate osteosynthesis: the effect of plate-to-bone compression with and without angular screw stability. J Orthop Trauma. 2007 Jul;21(6):362-8.
**22.** Bottlang M, Lesser M, Koerber J, Doornink J, von Rechenberg B, Augat P, Fitzpatrick DC, Madey SM, Marsh JL. Far cortical locking can improve healing of fractures stabilized with locking plates. J Bone Joint Surg Am. 2010 Jul 7;92 (7):1652-60.
**23.** Beingessner D, Moon E, Barei D, Morshed S. Biomechanical analysis of the less invasive stabilization system for mechanically unstable fractures of the distal femur: comparison of titanium versus stainless steel and bicortical versus unicortical fixation. J Trauma. 2011 Sep;71(3):620-4.
**24.** Döbele S, Horn C, Eichhorn S, Buchholtz A, Lenich A, Burgkart R, Nüssler AK, Lucke M, Andermatt D, Koch R, Stöckle U. The dynamic locking screw (DLS) can increase interfragmentary motion on the near cortex of locked plating constructs by reducing the axial stiffness. Langenbecks Arch Surg. 2010 Apr;395(4):421-8. Epub 2010 Apr 1.
**25.** Lacroix D, Prendergast PJ. Three-dimensional simulation of fracture repair in the human tibia. Comput Methods Biomech Biomed Engin. 2002b Oct;5(5):369-76.
**26.** Anderson DD, Thomas TP, Campos Marin A, Elkins JM, Lack WD, Lacroix D. Computational techniques for the assessment of fracture repair. Injury. 2014 Jun;45 (Suppl 2):S23-31.
**27.** Lujan TJ, Madey SM, Fitzpatrick DC, Byrd GD, Sanderson JM, Bottlang M. A computational technique to measure fracture callus in radiographs. J Biomech. 2010 Mar 3;43(4):792-5. Epub 2009 Nov 14.
**28.** US National Library of Medicine. The visible human project. 2015 Sep 21. https://www.nlm.nih.gov/research/visible/visible_human.html. Accessed 2015 Oct 19.
**29.** Marsh JL, Slongo TF, Agel J, Broderick JS, Creevey W, DeCoster TA, Prokuski L, Sirkin MS, Ziran B, Henley B, Audigé L. Fracture and dislocation classification compendium - 2007: Orthopaedic Trauma Association classification, database and outcomes committee. J Orthop Trauma. 2007 Nov-Dec;21(10)(Suppl):S1-133.
**30.** Comiskey DP, Macdonald BJ, McCartney WT, Synnott K, O'Byrne J. The role of interfragmentary strain on the rate of bone healing-a new interpretation and mathematical model. J Biomech. 2010 Oct 19;43(14):2830-4. Epub 2010 Jul 23.
**31.** Yamagishi M, Yoshimura Y. The biomechanics of fracture healing. J Bone Joint Surg Am. 1955 Oct;37(5):1035-68.
**32.** van der Vis H, Aspenberg P, de Kleine R, Tigchelaar W, van Noorden CJ. Short periods of oscillating fluid pressure directed at a titanium-bone interface in rabbits lead to bone lysis. Acta Orthop Scand. 1998 Feb;69(1):5-10.
**33.** Palomares KT, Gleason RE, Mason ZD, Cullinane DM, Einhorn TA, Gerstenfeld LC, Morgan EF. Mechanical stimulation alters tissue differentiation and molecular expression during bone healing. J Orthop Res. 2009 Sep;27(9):1123-32.

**34.** Loboa EG, Beaupré GS, Carter DR. Mechanobiology of initial pseudarthrosis formation with oblique fractures. J Orthop Res. 2001 Nov;19(6):1067-72.

**35.** Hayward LN, Morgan EF. Assessment of a mechano-regulation theory of skeletal tissue differentiation in an in vivo model of mechanically induced cartilage formation. Biomech Model Mechanobiol. 2009 Dec;8(6):447-55. Epub 2009 Jan 21.

**36.** Comiskey DP, MacDonald BJ, McCartney WT, Synnott K, O'Byrne J. Predicting the external formation of a bone fracture callus: an optimisation approach. Comput Methods Biomech Biomed Engin. 2012;15(7):779-85. Epub 2011 May 27.

**37.** Hagiwara Y, Dyment NA, Jiang X, Jiang Ping H, Ackert-Bicknell C, Adams DJ, Rowe DW. Fixation stability dictates the differentiation pathway of periosteal progenitor cells in fracture repair. J Orthop Res. 2015 Jul;33(7):948-56. Epub 2015 May 13.

**38.** DiGioia AM 3rd, Cheal EJ, Hayes WC. Three-dimensional strain fields in a uniform osteotomy gap. J Biomech Eng. 1986 Aug;108(3):273-80.

**39.** Paller DJ, Frenzen SW, Bartlett CS 3rd, Beardsley CL, Beynnon BD. A three-dimensional comparison of intramedullary nail constructs for osteopenic supracondylar femur fractures. J Orthop Trauma. 2013 Feb;27(2):93-9.

**40.** Augat P, Burger J, Schorlemmer S, Henke T, Peraus M, Claes L. Shear movement at the fracture site delays healing in a diaphyseal fracture model. J Orthop Res. 2003 Nov;21(6):1011-7.

**41.** Duda GN, Mandruzzato F, Heller M, Kassi JP, Khodadadyan C, Haas NP. Mechanical conditions in the internal stabilization of proximal tibial defects. Clin Biomech (Bristol, Avon). 2002 Jan;17(1):64-72.